A Scalable Reduced-Order Modeling Algorithm for the Construction of Parameterized Interconnect Macromodels from Scattering Responses

T. Bradde, S. Grivet-Talocia, M. De Stefano, A. Zanco
Dept. Electronics and Telecommunications, Politecnico di Torino
e-mail stefano.grivet@polito.it

***Abstract*—This paper introduces an algorithm for the construction of reduced-order macromodels of electrical interconnects starting from their sampled scattering responses. The produced macromodels embed in a closed-form an approximate dependence of the model equations on external parameters such as geometrical dimensions or material characteristics. The resulting parameterized models are easily cast as parameter-dependent SPICE netlists, which can be used for system-level Signal and Power Integrity assessment via numerical simulation, including sensitivity and optimization tasks. The main novel contribution of this work is the formulation of the model fitting equations in a decoupled form, which allows for a very efficient implementation in case of interconnects with a large number of interface ports, as typically required in Signal and Power Integrity applications. The parameterized models are guaranteed stable and passive for any configuration of the external parameters, thus ensuring stable transient numerical simulations.**

I. Introduction

The Signal and Power Integrity of electronic systems is strongly affected by the non-ideal behavior of electrical interconnects. Systematic numerical simulations are therefore required in both pre-layout and post-layout stages of the design. In a pre-layout setting, different system topologies and design scenarios are tested, leading to the choice of the final configuration that will be realized. During this phase, various what-if and optimization tasks are in order, so that the influence of all geometrical and possibly material parameters is taken into account while assessing the robustness of a particular configuration. Numerical simulation plays a crucial role in this phase: all decisions are driven by the results of some simulation task, from the electromagnetic field down to the circuit level.

During the past two decades, reduced-order behavioral macromodeling has become one of the leading approaches for bridging the gap between the electromagnetic characterization of interconnects and circuit-level description [1]. Starting from port responses such as sampled scattering data obtained from frequency-domain field solvers, a macromodeling tool computes a frequency-domain rational approximation of such responses while enforcing the stability and the passivity of the resulting model. The latter is then synthesized as an equivalent circuit, which can be run very efficiently by any SPICE solver for system-level Signal and Power Integrity assessment. In this framework, the Vector Fitting (VF) scheme [2], [3] is the standard choice, thanks also to the widespread availability of the algorithms both as open-source code and as commercial products integrated into EDA suites.

This work extends the idea of behavioral macromodeling by embedding in the models the dependence on one or more external parameters, such as geometrical dimensions or material characteristics. The model becomes multivariate, with one independent variable being frequency, and the other variables being the external parameters. Availability of such parameterized models opens new scenarios for system optimization, design centering and what-if analysis, which are parts of the daily work of a Signal and Power Integrity engineer. Such tasks would be greatly enhanced and simplified if fast and accurate models in a parameterized SPICE form were available.

The idea of parameterized (multivariate) macromodeling is not new [4]–[6]. However, a routine application of parameterized models in industrial workflows is still not adopted by design companies, since such parameterized models are not robust enough when compared to their non-parameterized VF-based counterpart. One can run into problems due to missing stability and passivity of the parameterized models for some parameter value, due to the fact that enforcing stability and passivity in the parameterized setting is orders of magnitude more difficult than in the non-parameterized case. Prototypal codes and research results are available [7], [8], but none of these results has made it so far in commercial EDA tools. Another difficulty is related to the scalability of the model generation algorithms: when the size of the input scattering data becomes large and especially when the number of ports of the interconnect to be modeled is large, no existing algorithm is capable of producing reliable models in a resonable time.

This paper makes one step forward towards the generation of reliable parameterized macromodels of interconnects, with emphasis on the efficiency of the model construction algorithm when a large number of ports is considered. We introduce and apply a decoupling approach based on a repeated QR factorization to the main least squares system for model identification [3]. The result is a numerical scheme that runs in linear time and memory with respect to the total number of port responses being concurrently processed. In addition, we are able to ensure that the parameterized model is stable for any parameter value within the considered range: although the model poles depend on the parameters, their real part is guaranteed to remain negative. Finally, a multivariate passivity enforcement scheme is applied to guarantee that the models are also uniformly passive throughout their parameter space. A preliminary description of the stability and passivity enforcement algorithms in the bivariate case are already available in [7], [8]. Therefore, we focus our presentation here on the decoupling process and its implementation. We start with a general problem statement and formulation in Sec. II. The decoupling scheme is detailed in Sec. III. Finally, Sec. IV illustrates the performance of the proposed algorithm on various interconnect examples.

II. Problem statement

We start with a P-port electrical interconnect structure characterized by its frequency-dependent scattering responses. We assume that these responses depend also on ρ additional parameters collected in a parameter vector $\vartheta \in \Theta \subset \mathbb{R}^\rho$. For instance, ϑ_1 could be the width of a transmission line, and ϑ_2 the dielectric permittivity of a substrate, etc. An initial characterization of the system response is first obtained via a parametric sweep of a frequency-domain field solver, obtaining a possibly large-sized set of response samples at discrete frequency and parameter values (s_k, ϑ_m), where $k = 1, \ldots, \bar{k}$ denotes frequency sampling ($s = j\omega$ is the Laplace variable) and $m = 1, \ldots, \bar{m}$ spans the parameter space through a global linear indexing. We denote these original $P \times P$ scattering matrix responses as $\breve{\mathbf{H}}_{k,m} = \breve{\mathbf{H}}(s_k; \vartheta_m)$.

Our objective is the construction of a reduced-order model whose scattering response $\mathbf{H}(s; \vartheta)$ approximates this data through

$$\mathbf{H}(s_k; \vartheta_m) \approx \breve{\mathbf{H}}_{k,m}, \quad k = 1, \ldots, \bar{k},\ m = 1, \ldots, \bar{m}. \quad (1)$$

The requirements on this model should be:

- the approximation error between model responses and raw data should be smaller than a given threshold δ at any frequency and parameter sample point, based on a suitable norm (this norm will be defined later);
- the model response should be a rational function of the complex frequency s, so that the dynamics of the model can be cast as Ordinary Differential Equations; the above should be true for any value of the parameters ϑ;
- the model poles should be functions of the parameters as $p = p(\vartheta)$; in addition, the model should be uniformly stable $\forall \vartheta \in \Theta$, i.e., the real part of each model pole should be negative for any parameter configuration;
- the model should be uniformly passive, in order to enable stable and reliable transient simulations;
- the model structure should enable its synthesis as a compact SPICE circuit, so that system-level simulations for Signal and Power Integrity assessment can be performed with any standard circuit solver.

The above requirements can be fulfilled if the model is cast in a *Parameterized Sanathanan-Koerner (PSK)* form [4], [9]

$$\mathbf{H}(s; \vartheta) = \frac{\mathsf{N}(s, \vartheta)}{\mathsf{D}(s, \vartheta)} = \frac{\sum_{n=0}^{\bar{n}} \sum_{\ell=1}^{\bar{\ell}} \mathbf{R}_{n,\ell}\, \xi_\ell(\vartheta)\, \varphi_n(s)}{\sum_{n=0}^{\bar{n}} \sum_{\ell=1}^{\bar{\ell}} r_{n,\ell}\, \xi_\ell(\vartheta)\, \varphi_n(s)}, \quad (2)$$

where $\mathbf{R}_{n,\ell} \in \mathbb{R}^{P\times P}$ and $r_{n,\ell} \in \mathbb{R}$ are the real-valued model coefficients. Two separate sets of basis functions are used in (2). Frequency dependence is captured by the standard partial fraction basis functions, as commonly adopted in the Vector Fitting (VF) scheme: $\varphi_0(s) = 1$ and $\varphi_n(s) = (s - q_n)^{-1}$ for $n > 0$, where q_n are fixed "basis poles", which are either real or occur in complex conjugate pairs [1], [2]). Parameter dependence is captured by expanding both numerator and denominator coefficients in terms of suitable multivariate basis functions $\xi_\ell(\vartheta)$ (here we use a tensor product of first-kind Chebychev polynomials). Note that $\ell = (\ell_1, \ldots, \ell_\rho)$ is a multi-index whose dimension depends on the number ρ of parameters. In the following, we will define $T = \prod_{i=1}^{\rho} \bar{\ell}_i$, which corresponds to the cardinality of the parameter-dependent basis. The model poles, which are the zeros of the denominator $\mathsf{D}(s, \vartheta)$, are therefore automatically (and implicitly) parameter-dependent, given that the parameterization is performed not directly on the poles but on the coefficients of the partial fractions. Note that (2) is the same starting point for the standard VF scheme (in the non-parametric case).

A. Model identification

The identification of the model coefficients in (2) is best achieved through the *PSK iteration* [4], [8], [9]. We start by initializing the denominator to a unit value $\mathsf{D}^0 = 1$, and we setup the following scheme, where superscripts denote estimates at iteration $\mu = 1, 2, \ldots$

$$\min \left\| \frac{\mathsf{N}^\mu(j2\pi f_k, \vartheta_m) - \mathsf{D}^\mu(j2\pi f_k, \vartheta_m)\, \breve{\mathbf{H}}_{k,m}}{\mathsf{D}^{\mu-1}(j2\pi f_k, \vartheta_m)} \right\| \quad (3)$$

where minimization is performed over the model coefficient estimates $\mathbf{R}^\mu_{n,\ell}$ and $r^\mu_{n,\ell}$. The cost function adopted in (3) is a user-defined norm of its $P \times P$ matrix argument, which can be tuned to the specific application scenario (see later). We recognize that (3) is a simple weighted linear least squares problem, whose solution is achieved through basic pseudoinverse techniques. The iteration terminates when the coefficient estimates stabilize. Note that, at convergence, the problem (3) coincides with the original model fitting requirement (1).

III. Handling large port counts

Despite its simplicity, the PSK iteration becomes intractable in its standard formulation (3) when the number of interconnect ports P is large. A straightforward calculation shows that the total number of unknowns that are being solved for in (3) is $N_c = (\bar{n} + 1)T(P^2 + 1)$, whereas the total number of constraints that are simultaneously imposed is $N_r = \bar{k}\bar{m}P^2$. The least-squares matrix $\mathbf{\Psi}$ of (3) has thus a size $N_r \times N_c$, which scales badly with the number of ports P of the interconnect under analysis. A closer look at this matrix, however, reveals a well-defined structure that we exploit to enhance the performance of the model identification, as discussed below.

Let us consider the model structure (2). We collect all the denominator coefficients $r_{n,\ell}$ in a column vector $\mathbf{d} \in \mathbb{R}^{(\bar{n}+1)T}$.

Any ordering of the tensor coefficients through a single global linear indexing scheme can be adopted, as far as this ordering is consistent throughout all derivations. Similarly, we collect all numerator coefficients corresponding to element (i,j) of the model response in a column vector $\mathbf{c}_{i,j} \in \mathbb{R}^{(\bar{n}+1)T}$. A row-vector $\mathbf{g}(s,\vartheta) \in \mathbb{C}^{1\times(\bar{n}+1)T}$ is then defined, whose elements collect the values of the multivariate basis functions $\xi_\ell(\vartheta)\,\varphi_n(s)$ at a generic point (s,ϑ). We now evaluate $\mathbf{g}(s,\vartheta)$ at the frequency and parameter values (s_k,ϑ_m) that are available from the original responses from the solver, and we stack all these vectors (with any suitable ordering) as rows of a matrix, which we denote as $\mathbf{\Phi} \in \mathbb{C}^{\bar{k}\bar{m}\times(\bar{n}+1)T}$. Collecting now all raw samples of the (i,j)-th response along the diagonal of matrix $\breve{\mathbf{H}}_{(i,j)}$ and stacking the corresponding values of $\{\mathsf{D}^{\mu-1}(\mathrm{j}2\pi f_k,\vartheta_m)\}^{-1}$ in a diagonal matrix $\mathbf{W}^{\mu-1}$, we obtain the compact matrix formulation of (3) as

$$\mathbf{\Psi}\mathbf{x} \approx \mathbf{0}, \tag{4}$$

where

$$\mathbf{\Psi} = \begin{pmatrix} \mathbf{\Gamma} & \mathbf{0} & \dots & \mathbf{0} & \mathbf{\Xi}_{(1,1)} \\ \mathbf{0} & \mathbf{\Gamma} & \dots & \mathbf{0} & \mathbf{\Xi}_{(2,1)} \\ \vdots & \vdots & \ddots & \vdots & \vdots \\ \mathbf{0} & \mathbf{0} & \dots & \mathbf{\Gamma} & \mathbf{\Xi}_{(P,P)} \end{pmatrix}, \quad \mathbf{x} = \begin{pmatrix} \mathbf{c}_{(1,1)} \\ \mathbf{c}_{(2,1)} \\ \vdots \\ \mathbf{c}_{(P,P)} \\ \mathbf{d} \end{pmatrix}, \tag{5}$$

and $\mathbf{\Gamma} = \mathbf{W}^{\mu-1}\mathbf{\Phi}$ and $\mathbf{\Xi}_{(i,j)} = -\mathbf{W}^{\mu-1}\breve{\mathbf{H}}_{(i,j)}\mathbf{\Phi}$. All these matrices are complex-valued, whereas the unknown vector $\mathbf{x}$ is real-valued.

Application of a standard QR-based least-squares solver [10] to the overdetermined system (4) would imply a matrix fill-in during the solution step, leading to a dramatic increase in memory occupation and requiring long runtime. However, the bordered block diagonal matrix structure in (5) enables a very efficient decoupling scheme. First, we compute the QR factorization

$$(\mathbf{\Gamma},\mathbf{\Xi}_\nu) = \mathbf{Q}_\nu\mathbf{R}_\nu = \mathbf{Q}_\nu \begin{pmatrix} \mathbf{R}_\nu^{11} & \mathbf{R}_\nu^{12} \\ \mathbf{0} & \mathbf{R}_\nu^{22} \end{pmatrix} \tag{6}$$

where ν denotes any pair (i,j) with $\nu = 1,\dots,P^2$. Once all the $\mathbf{R}_\nu^{22}$ blocks have been computed, we solve the least-squares system

$$\begin{pmatrix} \mathbf{R}_1^{22} \\ \mathbf{R}_2^{22} \\ \vdots \\ \mathbf{R}_{P^2}^{22} \end{pmatrix} \mathbf{d} \approx \mathbf{0}. \tag{7}$$

This procedure amounts to eliminating all the numerator unknowns in terms of the denominator unknowns in $\mathbf{d}$, which are the only unknowns that need to be solved concurrently, and which are the only unknowns that we need to compute in order to advance through the PSK iterations (3). We also remark that, since all diagonal blocks $\mathbf{\Gamma}$ are identical, the QR factorization can be further optimized by orthogonalizing the columns of $\mathbf{\Gamma}$ upfront, and using the result within a loop over ν in order to determine all blocks in (6). Details are omitted due to lack of space. At the end of the PSK iterations, the numerator coefficients are computed through another least squares system with multiple right-hand sides

TABLE I

COMPARISON OF ASYMPTOTIC CPU AND MEMORY COSTS (PER ITERATION) FOR THE STANDARD PSK AND THE PROPOSED FPSK SCHEMES. SEE TEXT FOR DETAILS.

	CPU cost	Memory cost
PSK	$k\bar{m}(\bar{n}+1)^2T^2P^6$	$2k\bar{m}(\bar{n}+1)TP^2(P^2+1)$
FPSK	$\bar{k}\bar{m}(\bar{n}+1)^2T^2P^2$	$(\bar{n}+1)^2T^2(P^2+4)+4\bar{k}\bar{m}(\bar{n}+1)T$

$$\mathbf{\Gamma}\mathbf{C} \approx \mathbf{B}, \tag{8}$$

where

$$\mathbf{C} = (\mathbf{c}_{(1,1)},\dots,\mathbf{c}_{(P,P)}) \tag{9}$$

$$\mathbf{B} = (-\mathbf{\Xi}_{(1,1)}\mathbf{d},\dots,-\mathbf{\Xi}_{(P,P)}\mathbf{d}). \tag{10}$$

The proposed decoupling scheme was proposed for the first time in [3], applied to the standard VF scheme. In this work, we are basically extending the same idea to the general multivariate (parameterized) modeling, where VF cannot be applied as is.

A. Computational savings

An asymptotic estimation of the number of floating point operations and memory occupation required by the standard PSK and the proposed decoupled scheme, henceforth denoted as Fast-PSK or FPSK scheme, can be carried out. The results are collected in Table I, which demonstrates that the proposed FPSK scheme is characterized both CPU and memory costs that scale linearly with the total number of responses being processed, i.e., as $O(P^2)$. Conversely, the CPU and memory cost of the standard PSK scheme scale as $O(P^6)$ and $O(P^4)$, respectively. These results demonstrate that only with the proposed decoupled FPSK scheme we can deal with realistic Signal or Power Integrity problems characterized by a possibly large number of ports P. We remark that additional CPU cost savings can be applied by distributing the P^2 QR factorizations on different CPU cores in parallel. This optimization is left for future investigations.

B. Weighting schemes and accuracy optimization

The above derivation of the FPSK scheme assumes that the matrix $\mathbf{\Gamma}$ in (5) is repeated identically along the main diagonal of $\mathbf{\Psi}$. This case occurs when the cost function that is minimized in (3) is the standard euclidean norm applied to evaluate the model vs data error for any response (i,j) of the system. In some cases, however, if may be necessary to use a different norm. For instance, when some responses are very small (such as crosstalk responses on loosely coupled interconnects), a relative error measure is more appropriate for an accurate characterization of such responses. This is readily achieved through an additional weighting factor $w_{k,m;i,j}$ that can be frequency-, parameter- and response-dependent. In case of a relative error minimization, we simply define this

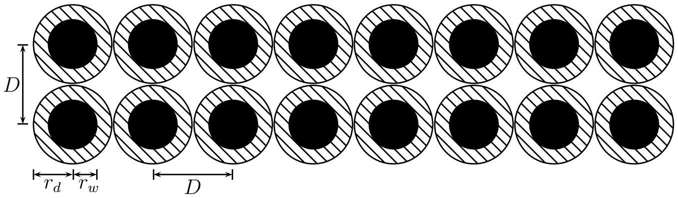

Fig. 1. Cross-section of the partially-coupled multiconductor interconnect (case of $M = 8$ differential pairs displayed).

weight as the inverse magnitude of the system responses. This weight is applied to every row in matrix $\mathbf{\Psi}$, obtaining a form similar to (5) but with all diagonal blocks now being different from each other. It can be shown that the scaling of CPU and memory cost with the number of ports P is the same as for the non-weighted FPSK scheme, but with a larger constant multiplier, since the QR factorization (6) has now to be performed in full for all independent blocks.

C. Enforcing model stability

We conclude this section by showing how the proposed decoupled FPSK scheme can be modified in order to enforce the stability of the parameterized model by construction. This is a fundamental requirement, since unstable models cannot be used for any practical application. Note that the stability requirement is far from being trival in the parameterized case, differently from the standard VF case [1], [2] where stability is enforced simply by ”flipping” the unstable poles (which are not parameterized). In the parameterized case, all the model poles are available as a post-processing from the model equations (by finding the zeros of the denominator in (2)). Without an explicit enforcement, there is no guarantee that these poles will be stable for any parameter value.

We solve this issue by exploiting a strong theoretical result. It can be proved [8] that the zeros of $\mathsf{D}(s, \vartheta)$ in (2) have a negative real part if the real part of $\mathsf{D}(s, \vartheta)$ is strictly positive for all frequencies $s = \mathrm{j}\omega$ and for all parameter values $\vartheta \in \Theta$. This condition basically corresponds to enforcing the denominator function $\mathsf{D}(s, \vartheta)$ to be a Positive Real function [1] for all ϑ. Since only the denominator is involved in this requirement, we are able to embed in the least-squares system (7) that is solved at each iteration a set of constraints $\mathrm{Re}\left\{\mathsf{D}(s_k, \vartheta_m)\right\} > \alpha$, where $\alpha > 0$ is a strictly positive constant. These constraints play the additional role of ruling out the trivial solution $\mathbf{d} = \mathbf{0}$, thus ensuring a well-behaved and well-conditioned model estimation process.

IV. Numerical results

We first consider a template interconnect problem, designed for testing the scalability properties of the proposed FPSK scheme when the number of interconnect ports increases. We consider a set of M differential pairs, each consisting of two parallel identical wires (conductor radius $r_w = 0.5$ mm, radius of dielectric insulation $r_d = 0.8$ mm with relative permittivity $\epsilon_r = 4.2$, center-to-center separation $D = 1.61$ mm). Each differential pair (vertically-oriented) is placed next to each other horizontally, as in Fig. 1, with all center-to-center separations of all wires equal to D. The number of pairs M ranges from 2 to 20, obtaining a number of (differential) ports P ranging from 4 to 40. This corresponds, in the largest case, to a total number of $P^2 = 1600$ responses that are concurrently fitted during model construction. The overall length of the interconnect is $L = 10$ cm. Each differential pair is considered to be an independent scalar transmission line over a length $L - L_c$, whereas over a length L_c all conductors are coupled forming a $2M$-wire multiconductor transmission line with differential ports. The coupling length $\vartheta = L_c$ is the free parameter for our multivariate model construction. Note that this parameter choice, due to the close vicinity of the conductors, induces very large variations in the scattering responses, making this an ideal test case for our algorithm.

For each value of M, we considered 11 linearly spaced values of L_c from 20 mm to 40 mm, and for each configuration we computed the scattering responses starting from the (frequency-dependent) per-unit-length matrices computed through an integral equation solver. This set of data was fed to the FPSK scheme. Some of the results are shown in Fig. 2, where various responses of the model for two different interconnect sizes are compared to the original scattering parameters for the entire set of L_c values. We see that the match is excellent, demonstrating that the model accuracy is not affected by the complexity of the structure under modeling. Fig. 3 shows instead the responses of a model constructed using a relative error norm. We see that the accuracy for small crosstalks is greatly enhanced with respect to the usual absolute error minimization.

The scalability of the proposed algorithm when increasing the number of ports P is demonstrated in Fig. 4, where both measured CPU times and their asymptotic estimates are compared. The linear dependence on the number of concurrently fitted responses for the FPSK is thus confirmed by the slope of the dashed lines. The figure shows also the measured and estimated cost of the standard PSK scheme applied to the same example. We see that, with respect to the asymptotic estimate, the adopted solver performs better. This is due to the sparsity of the least squares matrix in (5). However, even with this sparse solver, it was impossible to run a problem involving more than 6 ports due to memory requirements (although we used a server with 24 GB of memory).

We illustrate the robustness of the proposed approach by performing a parameterized transient SPICE run. An instance of the above-described coupled interconnect model with $P = 6$ ports was syntesized as a parameterized SPICE netlist [8]. The three near-end ports were closed in $2.5\,\Omega$ resistances, with the first line excited by a 2 V, single pulse (duration 1 ns, rise and fall times 200 ps). The far end ports were terminated into RC loads with two shunt overvoltage protection diodes. Transient results are displayed in Fig. 5, demonstrating that the proposed models (thanks to their uniform stability and passivity) run smoothly in any legacy circuit solver (we used LTSpice on a standard laptop, with a total runtime for the parametric transient sweep of 21 seconds).

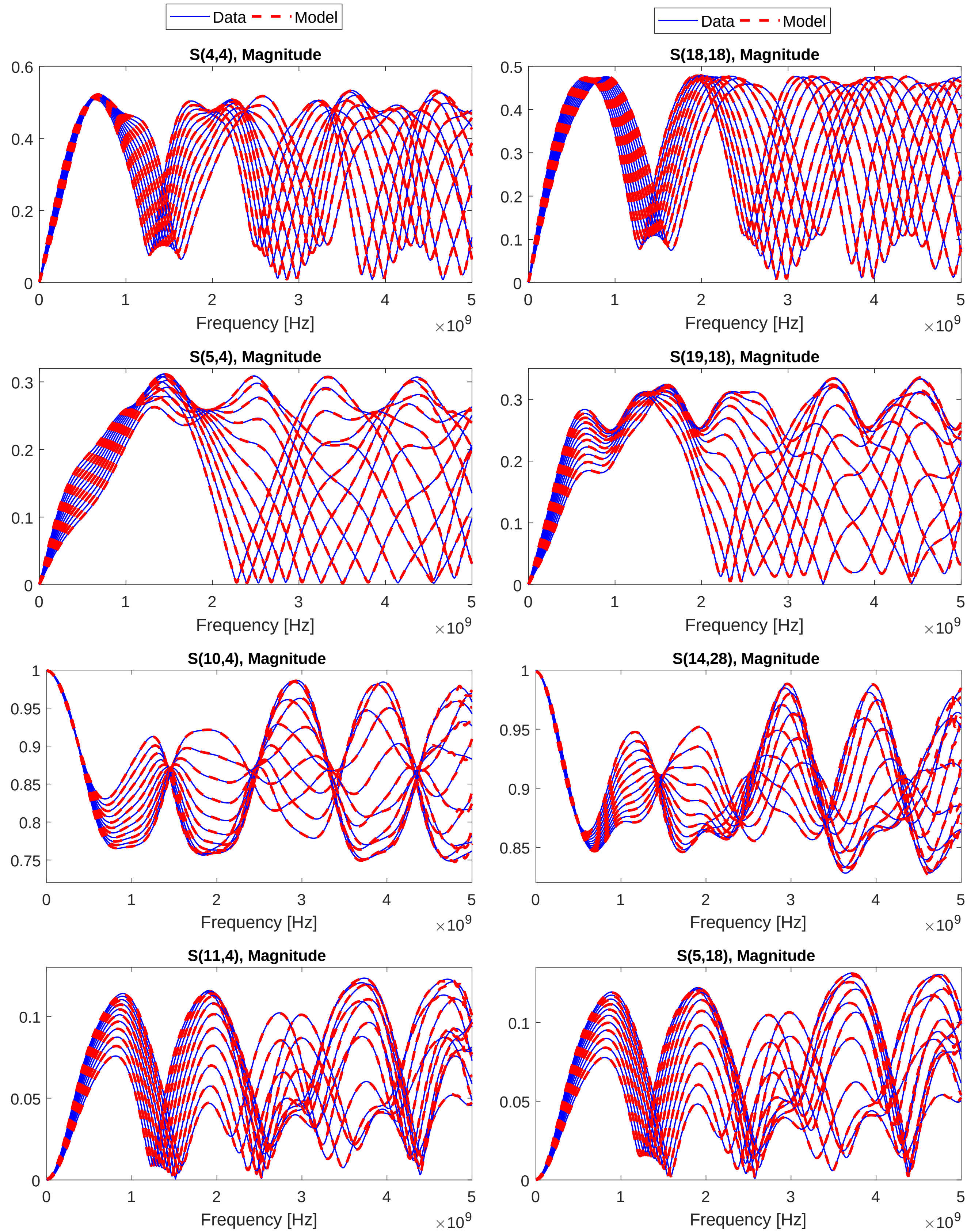

Fig. 2. Validation of selected parameterized model responses of the partially-coupled multiconductor line. Left panels: $P = 12$; right panels: $P = 28$.

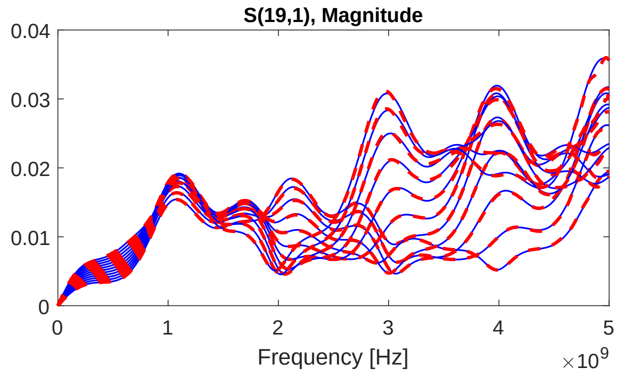

Fig. 3. Demostrating model accuracy for a small crosstalk response through relative error minimization.

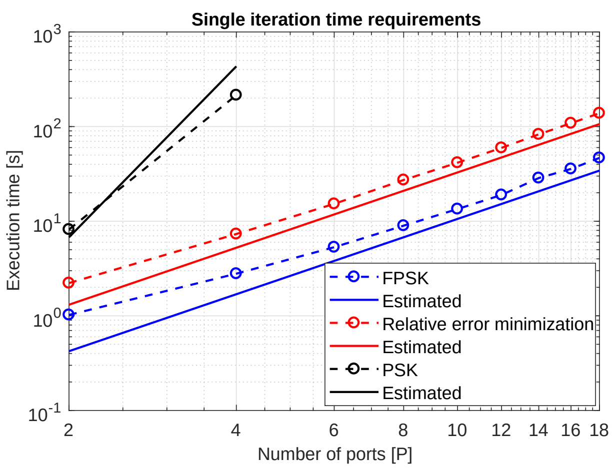

Fig. 4. Measured runtimes (dashed lines) and corresponding asymptotic estimates (solid lines) for PSK, FPSK, and FPSK with relative error minimization.

V. Conclusions

We presented an improved numerical scheme for the construction of behavioral macromodels of interconnect stuctures, including an explicit model dependence on additional parameters such as geometrical dimensions or material characteristics. The main objective of this research activity is to enable fast transient simulation for Signal and Power Integrity assessment via parameterized SPICE runs, including what-if, optimization and design centering.

Our new approach is based on a modification of a standard PSK scheme, based on a decoupling scheme through repeated QR factorizations. We demonstrated that the proposed FPSK scheme scales very favorably with the complexity of the interconnect under analysis, specifically in terms of total number of ports P. Therefore, we believe that the proposed formulation is the only existing parameterized macromodeling scheme that is able to deal with model extraction and macromodel-based simulation problems of practical industrial interest.

Our future research will investigate specialized data and model compression algorithms for dealing with structures characterized by many external parameters, with the main objective of circumventing the unavoidable curse of dimensionality induced by high-order parameter spaces.

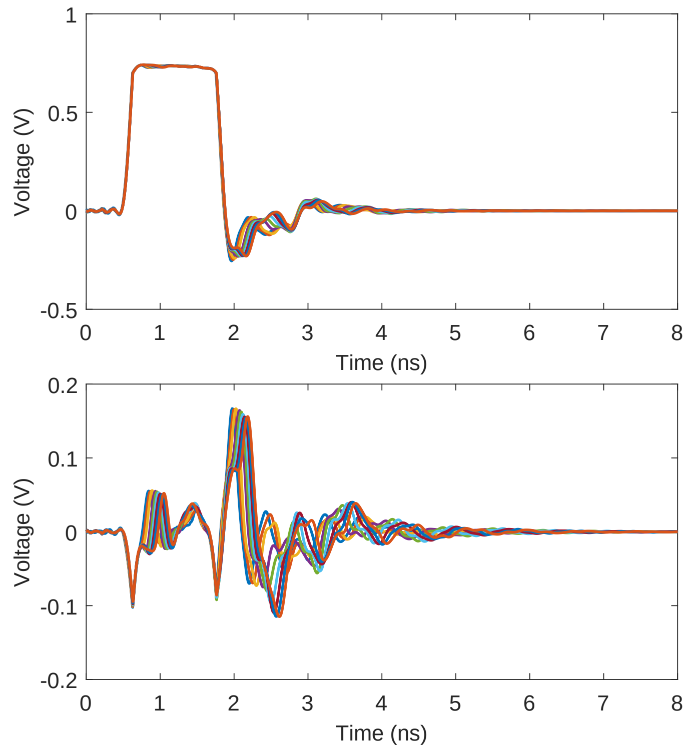

Fig. 5. Parametric transient analysis of a nonlinearly loaded interconnect model. Top panel: received signal; bottom panel: far end crosstalk voltage for different parameter configurations.

References

[1] S. Grivet-Talocia and B. Gustavsen, *Passive Macromodeling: Theory and Applications*. New York: John Wiley and Sons, 2016.

[2] B. Gustavsen, A. Semlyen, "Rational approximation of frequency domain responses by vector fitting", *IEEE Trans. Power Del.*, vol. 14, no. 3, pp. 1052-1061, July, 1999.

[3] D. Deschrijver, M. Mrozowski, T. Dhaene, and D. De Zutter, "Macromodeling of multiport systems using a fast implementation of the vector fitting method," *IEEE Microw. Wireless Comp. Lett.*, vol. 18, no. 6, pp. 383–385, Jun 2008.
macromodels of RF circuit blocks," *IEEE Trans. CPMT*, vol. 5, pp. 508-522, April 2015.

[4] P. Triverio, S. Grivet-Talocia, and M.S. Nakhla, "A Parameterized Macromodeling Strategy with Uniform Stability Test," *IEEE Transactions on Advanced Packaging*, vol. 32, no. 1, pp. 205-215, Feb. 2009.

[5] F. Ferranti, T. Dhaene, and L. Knockaert, "Compact and Passive Parametric Macromodeling Using Reference Macromodels and Positive Interpolation Operators," *IEEE Trans. CPMT*, vol. 2, no. 12, pp. 2080–2088, Dec. 2012.

[6] F. Ferranti, L. Knockaert, and T. Dhaene, "Passivity-Preserving Parametric Macromodeling by Means of Scaled and Shifted State-Space Systems," *IEEE Trans. MTT*, vol. 59, no. 10, pp. 2394–2403, Oct. 2011.

[7] S. Grivet-Talocia, "A Perturbation Scheme for Passivity Verification and Enforcement of Parameterized Macromodels", *IEEE Transactions on Components, Packaging and Manufacturing Technology*, vol. 7, pp. 18691881, Nov 2017.

[8] S. Grivet-Talocia, R. Trinchero, "Behavioral, Parameterized and Broadband Modeling of Wired Interconnects with Internal Discontinuities", *IEEE Transactions on Electromagnetic Compatibility*, vol. 60, pp. 7785, Feb 2018

[9] C. K. Sanathanan and J. Koerner, "Transfer function synthesis as a ratio of two complex polynomials," *IEEE Trans. Automatic Control*, vol. 8, no. 1, pp. 56–58, Jan. 1963.

[10] The Mathworks, Inc., www.mathworks.com. *MATLAB Users Guide.*